Electrochemistry Communications 11 (2009) 1830–1833

Contents lists available at ScienceDirect

Electrochemistry Communications

journal homepage: www.elsevier.com/locate/elecom

Glass–ceramic Li_2S–P_2S_5 electrolytes prepared by a single step ball billing process and their application for all-solid-state lithium–ion batteries

James Trevey, Jum Suk Jang, Yoon Seok Jung, Conrad R. Stoldt, Se-Hee Lee *

Department of Mechanical Engineering, University of Colorado, ECME 275, Boulder, CO, USA

ARTICLE INFO

Article history:
Received 3 June 2009
Received in revised form 25 July 2009
Accepted 27 July 2009
Available online 30 July 2009

Keywords:
Glass–ceramic
Mechanical ball milling
Li-ion conductivity
Si nanoparticle
Lithium–ion battery

ABSTRACT

We report that glass–ceramic Li_2S–P_2S_5 electrolytes can be prepared by a single step ball milling (SSBM) process. Mechanical ball milling of the $xLi_2S{\cdot}(100-x)P_2S_5$ system at 55 °C produced crystalline glass–ceramic materials exhibiting high Li-ion conductivity over 10^{-3} S cm^{-1} at room temperature with a wide electrochemical stability window of 5 V. Silicon nanoparticles were evaluated as anode material in a solid-state Li battery employing the glass–ceramic electrolyte produced by the SSBM process and showed outstanding cycling stability.

1. Introduction

Research on all-solid-state rechargeable lithium–ion batteries has increased considerably in recent years due to raised concerns relating to safety hazards such as solvent leakage and flammability of liquid electrolytes used for commercial lithium–ion batteries [1–7]. As solid state electrolytes by nature, do not carry the safety burdens of liquid electrolytes, an extensive worldwide effort is under way to produce a viable solid electrolyte to replace conventional liquid electrolytes. Beyond the obvious safety advantages of solid electrolytes, all-solid-state batteries can be constructed with a wide variety of solid electrolyte materials, vary in form and design, and have high reliability [4,8–10]. Unfortunately current research has yet to unveil a solid state electrolyte that can out perform liquid electrolyte. Inferior rate capability, low ionic conductivity, interfacial instability, and low loading of active materials are just a few of the barriers that stand in the way of the commercialization of all-solid-state rechargeable lithium–ion batteries [4,5]. Ideally, liquid electrolytes will be replaced by solid state electrolytes that perform similarly without excessive safety issues [11].

While melt and quench methods for $xLi_2S{\cdot}(100-x)P_2S_5$ binary system have produced promising results in the past, ball milling has emerged as a more enticing method for solid state electrolyte development because it is relatively lower cost and less time consuming [12]. Conventional ball milling techniques have proven useful for generating ultra-fine amorphous materials at room temperature. Fine powders function well for achieving high ionic conductivities as well as close contact between electrolytes and electrode materials for all-solid-state cells [1,2]. Ball milling has also proven effective for enlarging the compositional region in which amorphous materials are obtained, beyond that of conventional melt–quenching methods [7,13]. Ball milled amorphous powders are often heat treated to attain a crystalline structure capable of even higher conductivities than those reached by amorphous powders. Heat treatment of glass samples to a crystalline glass–ceramic state has shown to increase conductivity [9,14]. While effective, this multi-step process is time consuming and inefficient. More importantly, the post heat treatment usually results in glass–ceramic materials with larger particle size of which morphology is not desirable for use in all-solid-state Li-ion batteries. Here we report on glass–ceramic $xLi_2S{\cdot}(100-x)P_2S_5$ binary system produced by a single step ball milling (SSBM) process in terms of its structural and electrochemical characteristics. Using the glass–ceramic electrolytes developed by the SSBM technique, we have evaluated silicon nanoparticles as an anode material for use in all-solid-state Li-ion batteries. To our best knowledge, this is the first report on the application of Si nanoparticle as anode material for all-solid-state battery applications.

2. Experimental

Reagent-grade powders of Li_2S (Aldrich, 99.999%) and P_2S_5 (Aldrich, 99%) were used as starting materials for mechanical ball milling. Appropriate concentrations of materials were combined

* Corresponding author. Tel.: +1 303 492 7889; fax: +1 303 492 3498.
E-mail address: sehee.lee@colorado.edu (S.-H. Lee).

1388-2481/$ - see front matter © 2009 Elsevier B.V. All rights reserved.
doi:10.1016/j.elecom.2009.07.028

into a zirconia vial (Spex) at a net weight of one gram with two zirconia balls (1 × 12 mm, 1 × 15 mm in diameter) for grinding. High energy ball milling (Spex2000) took place for 20 continuous hours in an Ar-filled glove box at 55 °C. Ambient temperature was maintained by use of a temperature controller connected to a heater within the glovebox where ball milling took place. Ball milled vials were paused periodically to measure the vial temperature and adjust the ambient temperature accordingly to achieve desired vial temperature. A direct correlation was developed for the discrepancy between ambient and vial temperature and vials were then milled without pausing. High energy ball milling was also performed at room temperature. In order to maintain room temperature, vials were milled in 30 min intervals. By milling for 30 min and resting for 30 min repeatedly, temperatures can be held below at 32 °C for the 20 h milling time. Materials ball milled at room temperature were amorphous and their conductivity values were consistent with previously reported data [14]. Materials are then cold pressed (5 metric tons) into pellets 13 mm in diameter and 1 mm thick in a titanium die. The obtained samples were characterized by X-ray diffraction measurements with Cu-Kα radiation. Sample materials were sealed in an airtight aluminum container with beryllium windows and mounted on the X-ray diffractometer (PANalytical, PW3830). Diffraction measurements were observed for all starting materials as well as significant compositions between 10° and 40°. Ionic conductivities were measured by AC impedance spectroscopy (Solartron 1280C) for all SSBM sample materials. Weighed materials are cold pressed at 8 metric tons, before lithium metal plates are pressed to both sides of the pellet at 1 metric ton to serve as electrodes. The impedance of selected cells was measured from 20 to 100 mHz at room temperature and the conductivity was determined using complex impedance analysis.

For the galvanostatic charge–discharge cycling of liquid electrolyte lithium batteries, the composite electrode was prepared by spreading a slurry mixture of Si nanoparticles (50–100 nm, Alfa Aesar), acetylene black (AB, carbon additive for conductivity enhancement), and carboxymethyl cellulose (CMC, Aldrich, M_w = 90,000, DS = 0.70) (8:1:1 weight ratio) on a Cu foil. The galvanostatic charge–discharge cycling was performed with a two-electrode 2032-type coin cell in the potential range of 0.005–1.500 V (vs. Li^+/Li) at a current density of 200 mA g^{-1} at room temperature. Li foil was used as the counter electrode. About 1.0 M $LiPF_6$ dissolved in a mixture of ethylene carbonate (EC) and dimethyl carbonate (DMC) (1:1 v/v) was used as the electrolyte. Porous 20 μm thick polypropylene (PP)/polyethylene (PE)/PP tri-layer film was used as the separator.

The all-solid-state battery was fabricated as follows. The Si nanopowder, AB, and glass–ceramic electrolyte ($xLi_2S{\cdot}(100-x)P_2S_5$ (x = 77.5)) with a weight ratio of 1:1:5 were mixed using agate mortar and pestle to prepare composite working electrodes. A Li foil (0.75 mm thick) was used as the counter electrode. A bi-layer pellet comprising the working electrode (2 mg) and glass–ceramic electrolyte (150 mg) was obtained by pressing less than 5 metric tons. The Li foil was attached on the glass–ceramic electrolyte of bi-layer pellet under 1.5 metric tons. The pellet (φ = 1.3 cm) was pressed in a polyaryletheretherketone (PEEK) mold by two Ti-alloy rods which act as current collectors for working and counter electrodes. All processes were performed in an Ar-filled dry glove box. The galvanostatic charge–discharge cycling was performed in the potential range of 0.005–1.500 V (vs. Li/Li^+) at a current density of 210 mA g^{-1} at room temperature.

3. Results and discussion

Fig. 1 shows the X-ray diffraction (XRD) spectra of the glass–ceramic samples in the composition range $70 < x < 80$ for

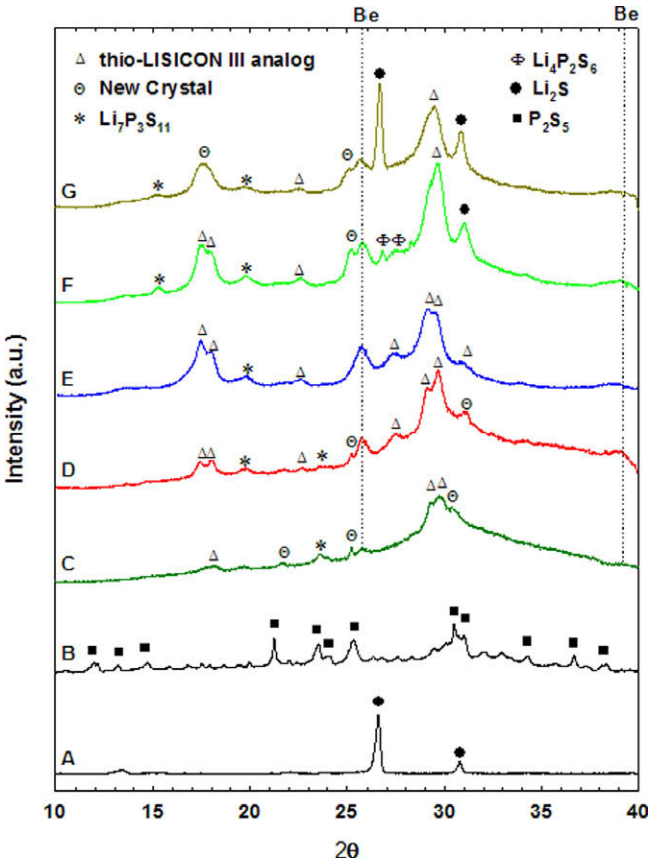

Fig. 1. XRD patterns for all tested electrolytes, (A) Li_2S, (B) P_2S_5, (C) x = 70, (D) x = 72.5, (E) x = 75, (F) x = 77.5, and (G) x = 80.

$[xLi_2S{\cdot}(100-x)P_2S_5]$. Sharp diffraction peaks are observed among all compositions due to the crystalline material structure formed under the SSBM method. For concentrations of x = 77.5 and x = 80 electrolytes sharp diffraction peaks are observed near 25.5° and 31° due to excess Li_2S content in the sample [2,11]. The diffraction patterns for SSBM samples show a trend of increasing intensity of crystalline peaks up to x = 77.5 at which point only the Li_2S peaks intensify for x = 80. Formation of a new crystalline phase similar in structure to that of thio-LISICON II analog can be observed by similarly positioned peaks throughout the composition range [2]. Individual properties of compounds such as the low melting temperature of P_2S_5 may be a factor in the crystallization of materials during SSBM.

Fig. 2a shows a conductivity map comparing the conductivity values attained from our amorphous glass and SSBM glass–ceramic electrolytes with Tatsumisago groups' amorphous glass and two step glass–ceramic samples [14]. Standard two step heat treatment shows increased conductivities over glass electrolytes caused by formation of new highly conductive crystalline structures [14]. For the SSBM glass–ceramics, enhancement in conductivity by crystallization was due to formation of a highly conductive crystalline phase during the ball milling process, analogous to the thio-LISICON phase $Li_{4-x}Ge_{1-x}P_xS_4$ ($0.6 < x < 0.8$) defined by a unique monoclinic superstructure exhibiting high conductivities over 10^{-3} S cm^{-1} [15]. We found that the values for conductivity attained by SSBM were higher by approximately one order of magnitude than all glass electrolytes and were as high as or higher than those values for glass–ceramics by standard two step heat treatment for all but the compositions at the extremes of our range [14]. The SSBM glass–ceramic sample with x = 70 was not as high as standard two step glass–ceramics, but the SSBM glass–ceramic

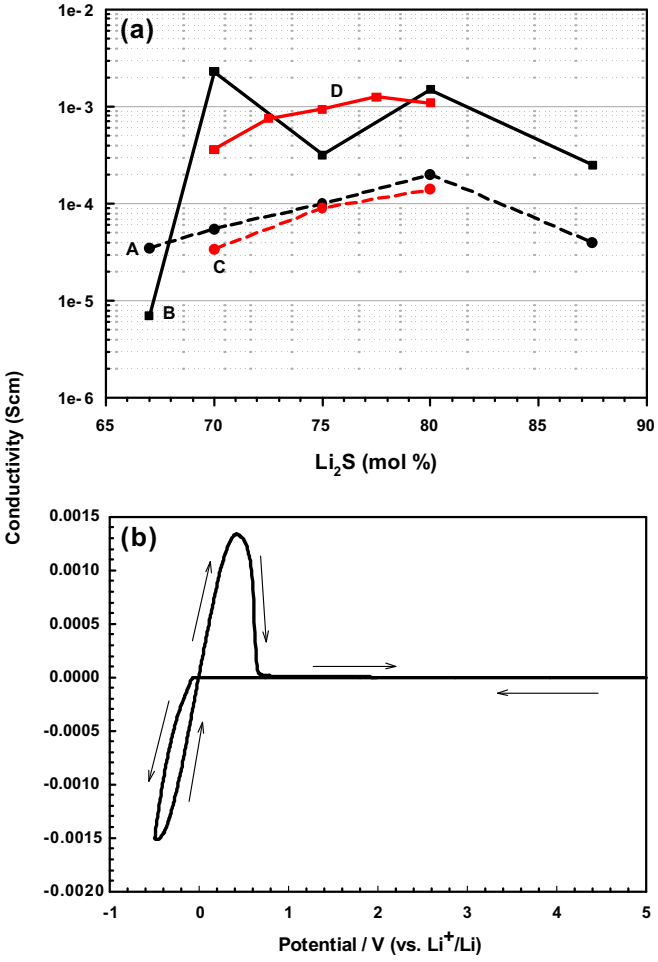

Fig. 2. (a) Conductivity map for $[xLi_2S{\cdot}(100-x)P_2S_5]$ (mol.%) for $70 < x < 80$ (A) glass[14], (B) glass–ceramic[14], (C) our glass, (D) SSBM glass–ceramic. (b) The stability window for the first cycle of tested SSBM glass–ceramic sample $x = 72.5$. Glass–ceramic samples containing larger concentrations of Li_2S are not shown but follow a similar trend as the other samples with a maximum recorded current of 0.0144 μA for $x = 80$. Repeated cycling shows a negligible difference in the stability windows of all samples.

sample with $x = 80$ was comparably close in conductivity to the standard two step glass–ceramic sample. We attribute this discrepancy in conductivities for $x = 70$ to the lower temperature at which SSBM samples are exposed in comparison to standard heat treating. We speculate the entire SSBM conductivity curve can rise as a result of higher ball milling temperatures. More systematic studies on the effect of the ball milling temperature on ionic conductivity are in progress. The simplicity of the SSBM process and high ionic conductivity of SSBM samples make the SSBM method superior for development of solid state electrolytes for all-solid-state battery production. Furthermore, the SSBM with no post heat treatment required, completely eliminates any potential grain growth of as-ball-milled fine powders.

Fig. 2b shows stability window for samples tested with titanium rod and lithium foils as the working and counter electrodes, respectively. Measurements were carried out from the rest potential to the cathodic direction and then the anodic direction up to 5 V vs. Li^+/Li and down to −0.5 V vs. Li^+/Li. No reactions were observed in these voltammograms except for lithium deposition ($Li^+ + e^- \rightarrow Li$) and dissolution ($Li \rightarrow Li^+ + e^-$) reactions between −0.5 and 0.6 V, up to 5 V vs. Li^+/Li, suggesting that the SSBM materials have a wider electrochemical window than 5 V [7].

Using the glass–ceramic electrolytes produced by the SSBM technique, silicon nanoparticles were evaluated as anode material for use in all-solid-state Li-ion batteries. Fig. 3a shows the charge and discharge curves of all-solid-state cells fabricated using Si nanoparticles as the anode material and solid electrolyte $xLi_2S{\cdot}(100-x)P_2S_5$ ($x = 77.5$) as solid electrolyte. The battery cell was cycled between 0.005 and 1.5 V vs. Li^+/Li at a current density of 210 mA g^{-1} at room temperature. To our best knowledge, this is the first demonstration of an all-solid-state battery using Si nanoparticles. The first charge and discharge capacities of Si nanoparticles were found to be 3127 and 1367 mAh g^{-1}, respectively. During the first cycle (Fig. 3a), the potential rapidly drops to 1.0 V, stays at ~1.0 V showing a small plateau, and then gradually drops to 0.005 V. After the first cycle, the charge and discharge capacities in the subsequent cycles are highly reversible as shown in Fig. 3b.

Fig. 3b compares the cycling performance of solid state and liquid electrolyte systems employing Si nanoparticles. The charge capacity of solid glass–ceramic electrolyte system decreases very slowly from 1420 to 950 mAh g^{-1} up to the 40th cycle. The Si nanoparticles in solid-state battery configuration exhibited a capacity retention of 66.9% after 40 charge–discharge cycles in the 0.005–1.5 V (vs. Li/Li^+) range. In contrast, the Si nanoparticles in conventional liquid electrolyte cell displayed only 14% capacity retention. This difference in capacity retention with respect to cy-

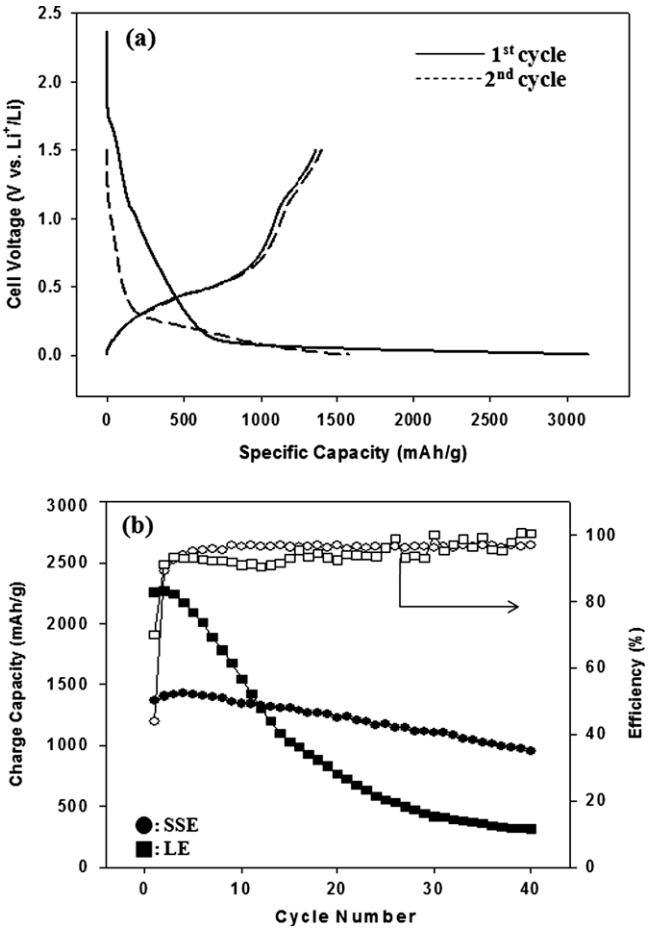

Fig. 3. (a) The charge and discharge curves of all-solid-state cell fabricated with Si nanopowder as anode material and solid electrolyte $xLi_2S{\cdot}(100-x)P_2S_5$ ($x = 80$) as solid state electrolyte. The cell was cycled between 0.005 and 1.5 V at a current density of 210 mA g^{-1}. (b) The cycle performance of solid state electrolyte (SSE, ●) and liquid electrolyte (LE, ■) lithium battery cells fabricated using Si nanoparticles. Open circle (○) and rectangle (□) correspond to the coulombic efficiencies of solid state electrolyte (SSE) and liquid electrolyte (LE) cells, respectively.

cling is related to the volume expansion during Li accumulation. It is well known that the volume change of Li–Si alloy is approximately 400% when 1 mol Si absorbed 4.4 mol Li in lithium secondary battery with a liquid electrolyte [16–18]. In contrast, it is believed that the volume change as well as cracking of the Si nanoparticles in solid-state lithium battery cell could be much less than liquid electrolyte lithium batteries because of the pelletized active mixture and strong built-in pressure in the solid-state cell [19]. Fig. 3b also shows the coulombic efficiency of the two systems. The decrease in efficiency during the 1st and 2nd cycles is due to the irreversible alloying reaction. The coulombic efficiency of the solid-state cell shows stable values near 98% after three cycles. On the other hand, the liquid electrolyte cell shows unstable values in the range of 91–95%.

4. Conclusions

Glass–ceramic solid state electrolytes were prepared from high energy ball milling of the $[x\mathrm{Li_2S}\cdot(100-x)\mathrm{P_2S_5}]$ system with simultaneous heating called SSBM. Electrolytes of the concentration $77.5\mathrm{Li_2S}$–$22.5\mathrm{P_2S_5}$ mol.% proved to have the best overall conductivity, displaying an ionic conductivity of 1.27×10^{-3} S cm^{-1} at room temperature. The data obtained from XRD measurement provided validation for the production of a crystalline glass–ceramic electrolyte from a one step process. Si nanoparticles were evaluated as anode material in all-solid-state batteries using glass–ceramic solid electrolytes prepared by the SSBM technique and showed outstanding cycling stability. To the best of our knowledge this is the first demonstration of Si nanoparticles as an anode material for lithium–ion batteries, and as such, optimization of liquid and solid state electrode composition and construction is ongoing. Further studies are required to fully understand and overcome the irreversible capacity loss during the initial cycle.

Acknowledgments

This work has been supported by DARPA/DSO.

References

[1] A. Hayashi, S. Hama, F. Mizuno, K. Tadanaga, T. Minami, M. Tatsumisago, Solid State Ionics 175 (2004) 683.
[2] A. Hayashi, S. Hama, T. Minami, M. Tatsumisago, Electrochem. Commun. 5 (2003) 111.
[3] N. Ohta, K. Takada, I. Sakaguchi, L. Zhang, R. Ma, K. Fukuda, M. Osada, T. Sasaki, Electrochem. Commun. 9 (2007) 1486.
[4] Y. Hashimoto, N. Machida, T. Shigematsu, Solid State Ionics 175 (2004) 177.
[5] K. Takada, T. Inada, A. Kajiyama, M. Kouguchi, H. Sasaki, S. Kondo, Y. Michiue, S. Nakano, M. Tabuchi, M. Watanabe, Solid State Ionics 172 (2004) 25.
[6] K. Takada, T. Inada, A. Kajiyama, H. Sasaki, S. Kondo, M. Watanabe, M. Murayama, R. Kanno, Solid State Ionics 158 (2003) 269.
[7] N. Machida, H. Yamamoto, S. Asano, T. Shigematsu, Solid State Ionics 176 (2005) 473.
[8] F. Mizuno, A. Hayashi, K. Tadanaga, M. Tatsumisago, Solid State Ionics 177 (2006) 2731.
[9] M. Tatsumisago, Solid State Ionics 175 (2004) 13.
[10] S. Kondo, K. Takada, Y. Yamamura, Solid State Ionics 53 (1992) 1183.
[11] F. Mizuno, A. Hama, A. Hayashi, K. Tadanaga, T. Minami, M. Tatsumisago, Chem. Lett. (2002) 1244.
[12] A. Hayashi, S. Hama, H. Morimoto, M. Tatsumisago, T. Minami, J. Am. Ceram. Soc. 84 (2001) 477.
[13] H. Yamamoto, N. Machida, T. Shigematsu, Solid State Ionics 175 (2004) 707.
[14] M. Tatsumisago, F. Mizuno, A. Hayashi, J. Power Sources 159 (2006) 193.
[15] R. Kanno, M. Murayama, J. Electrochem. Soc. 148 (2001) A742.
[16] N. Yabuuchi, T. Mutoh, T. Ohzuku, Abstracts of the 44th Battery Symposium in Japan, 2003, p. 438.
[17] M. Miyachi, H. Yamamoto, H. Kawai, T. Ohta, M. Shirakata, J. Electrochem. Soc. 152 (2005) A2089.
[18] Y. Liu, Z. Wen, X. Wang, X. Yang, A. Hirano, N. Imanishi, Y. Takeda, J. Power Sources 189 (2009) 480.
[19] T. Jiang, S.C. Zhang, X.P. Qiu, W.T. Zhu, L. Chen, Electrochem. Commun. 9 (2007) 930.